〔研究〕

Structural Analyses of MBE Grown Cubic and Hexagonal GaN Epilayers by X-ray Diffraction

K. BALAKRISHNAN P. FONS H. OKUMURA S. YOSHIDA

Detailed X-ray analyses have been carried out on the epilayers of cubic and hexagonal GaN grown on (001) GaAs and (0001) sapphire substrates, respectively, by plasma assisted molecular beam epitaxy (MBE). In order to study the existence of secondary crystallographic phases in the cubic GaN epilayers, X-ray pole figures were generated on (001) surfaces of the samples. The exact locations of misoriented cubic and secondary hexagonal phases have been identified and their relative intensities were estimated. Threading dislocations were observed despite the exhibition of excellent structural properties by the hexagonal GaN epilayers as measured by high resolution X-ray diffraction. A comparison of crystal coherence and mosaicity for the epilayers grown under different growth conditions has been made. A possible explanation is given for the poor electrical characteristics exhibited by the structurally high quality epilayers.

§1 Introduction

Group III-nitride semiconductors have received lot of attention due to the successful demonstrations of high efficiency blue light emitting diodes (LEDs) and laser diodes (LDs)[1-3]. Due to the improvement in the quality of nitrogen source used for the MBE growth of group III nitrides, especially GaN, there has been lot of progress in the growth rate, structural, optical and electrical properties[4-6]. To date, most of the GaN based devices have been made of hexagonal phase. However, the cubic crystal of GaN offers several advantages over its hexagonal counterpart, namely easy cleavage, no columnar growth which makes it suitable for laser structures, lower phonon scattering and so on[7]. Also, according to theoretical predictions, the cubic phase of GaN should possess superior electronic properties for some device applications [8]. It is also hoped that the cubic nitrides may be more amenable to p-type doping[9].

However, unlike most of the other III-V compounds, the hexagonal phase is more stable than the cubic phase in the case of nitrides[10]. As a result, there is an increased tendency of forming hexagonal phase subdomains within the cubic lattice. The cubic GaN is usually grown on (001) surfaces of cubic substrates. However, a cubic substrate alone does not guarantee the stabilization of the cubic phase for the epilayers on it. By using transmission electron microscope (TEM) analysis, Yi Xie et al. have found the coexistence of three structural phases, i.e., wurtzite, zincblende and rocksalt, in their powder samples of GaN, prepared through benzene thermal reaction of Li_3N and $GaCl_3$ under high pressure[11]. Tsuchiya et al. have estimated the ratio of cubic to hexagonal components of GaN epilayers grown by hydride vapor phase epitaxy (HVPE) with the help of quantitative consideration of X-ray diffraction (XRD) intensities[12]

Sakai et al have studied the existence of hexagonal phase in the cubic GaN epilayers grown on (100) GaAs wafers by HVPE by TEM[13]. However the number of studies on the secondary phases present in nitride epilayers by X-ray diffraction has been very limited. Yamaguchi et al have analyzed their VPE grown hexagonal GaN epilayers on GaAs by doing θ-2θ scans for various lattice planes by inclining the sample continuously using 4-circle X-ray diffractometer[14]. Barring a very few reports, like the one by Yamaguchi et al, in most of the other studies by XRD, only θ-2θ scan has been performed without inclining the sample for assessing the secondary hexagonal crystallographic phases, but this gives in-

KEY WORDS : Ⅲ-nitride Semiconductors, phase mixing, structural properties, X-ray diffraction

formation only on the crystallographic planes parallel to the surface of the sample being analyzed. On the other hand, an X-ray pole figure generated on an epilayer gives a complete picture of the different structural phases present in it.

An X-ray pole figure gives the scattered intensity as a function of both Ψ and ψ axes, as shown in Fig.1. X-ray pole figures are generated by rotating the sample along ψ axis at different Ψ positions for a particular Bragg diffraction condition corresponding to the crystallographic plane being investigated (ω and 2θ values corresponding to the particular Bragg diffraction are kept constant). The diffracted intensities are presented on a Wulff projection, from which the orientation of the particular crystallographic planes being investigated can be worked out. For a complete pole figure, Ψ varies from 0 to 90° and ψ varies from 0 to 360° for each value of Ψ .

In spite of the progress achieved in the structural and electrical properties of the epilayers of hexagonal group III nitride semiconductors, there is still lot of work to be done to understand the structure and generation of defects and their relationship to physical properties, especially, electrical characteristics. Symmetric and asymmetric X-ray rocking curves are often used to study mosaic and therefore, indirectly, the dislocation content in the epilayers of GaN and related materials[15-17]. We have found that often hexagonal GaN epilayers exhibiting structurally outstanding properties are not always the best materials for electrical properties.

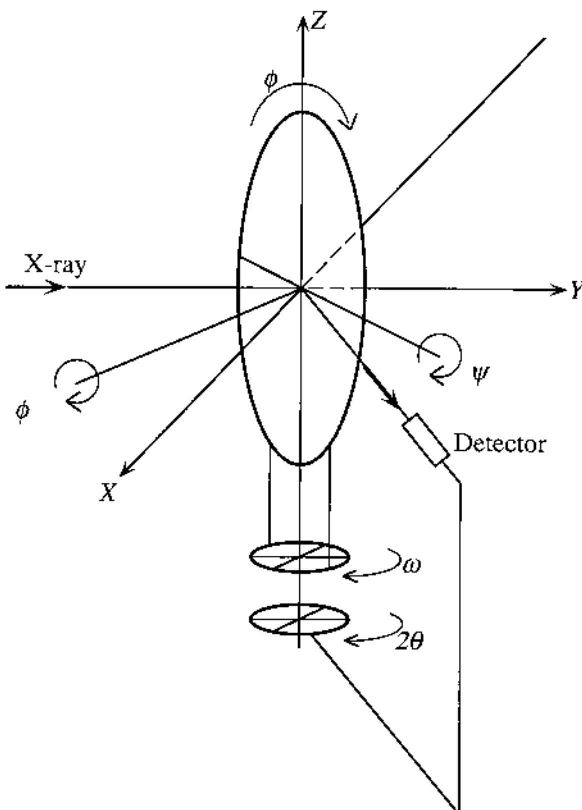

Fig.1 Different axial movements used for generating X-ray pole figures.

In the present investigation, we have studied the crystallographic structure of cubic GaN epilayers grown on (001) GaAs substrates and made an attempt to find out where the secondary hexagonal and misoriented cubic grains originate from. The usefulness of X-ray pole figure technique in accurately identifying the location of different structural phases, especially secondary phases, is shown. In addition we have studied in detail their structural properties of hexagonal GaN epilayers grown on (0001) sapphire substrates by high resolution X-ray diffraction (XRD) and Transmission electron microscopy (TEM). We have also tried to correlate the structural properties to the measured electrical characteristics.

§ 2 Experimental

2.1 Growth of cubic GaN

Cubic GaN epilayers were grown on (001) GaAs substrates by molecular beam epitaxy (MBE) technique. The MBE chamber was equipped with a turbomolecular pump and a cryopump in addition to a sputter ion pump. An ECR plasma nitrogen source was used for supplying nitrogen radicals. A constant nitrogen flow rate of 2 ccm was used and the growth temperature was kept at 630°C. Different values of the ECR power in the range from 40 W to 150 W were used, keeping other growth parameters constant. Prior to the cubic GaN nucleation, a GaAs layer was grown at 550°C for 3 minutes in order to get a smooth surface of GaAs. After this procedure, a GaN buffer layer was grown at 400°C for 3 minutes and then the substrate temperature was increased to the growth temperature. Cubic GaN epilayer was grown on this layer. Growth rate of the epilayers was approximately 10 Å per minute. Typical thickness of the samples used for the present investigation was approximately 2500 Å

Surface structures of the samples were monitored by reflection high energy electron diffraction (RHEED) during the growth.

2.2 Growth of hexagonal GaN

Hexagonal GaN epilayers have been grown on c-plane sapphire by MBE using RF nitrogen plasma. Sapphire substrates were degreased by acetone and methanol followed by etching in a solution of H_2SO_4: H_3PO_4 (1:1) for 10 minutes at 180°C. Surface structures were monitored by reflection high energy electron diffraction (RHEED) in situ. Nitrogen flow rate and plasma power were 2 sccm and 400 W, respectively. Different growth initiation processes, namely, nitridation, low temperature buffer layer growth of GaN and AlN have been done prior to the main growth of hexagonal GaN epilayers. During the nitridation, temperature of the substrate was slowly increased from 480°C to growth temperature. Growth temperatures were in the range 700°C-850°C. After carrying out the growth initiation as mentioned above, a process namely Nitrogen flux modulation process (NFM) was carried out during the first few minutes of the main growth of GaN, in order to flatten the epilayer surface. NFM was accomplished by operating the shutter of the nitrogen plasma source repeatedly keeping the Ga shutter open all the time. This was done for 5-10 minutes depending on the RHEED pattern observed. Typical growth rate achieved for the hexagonal GaN epilayers was 0.5 μm per hour.

2.3 X-ray diffraction

X-ray diffraction measurement was performed using a MAC Science 18,000 watt rotating anode Cu target. For generating pole figures, pin hole (exit slit) configuration was used with CuKa radiation. A solar slit was placed in front of the detector. In order to study the existence of secondary crystallographic phases in the cubic GaN epilayers, pole figures were generated on the sample surfaces. In the pole figure analysis, step sizes used in both Ψ and ψ movements were 0.1 degree. The counting periods were varied from 30 seconds to 180 seconds per step depending on the accuracy requirement of a particular scan.

High resolution X-ray diffraction was performed on the hexagonal GaN epilayers. A Phillips MRD diffractometer with a 4-bounce Ge(220) monochromator was used to select CuK α_1 radiation (λ = 1.540981 Å). Using triple-axis X-ray diffraction mode, the detector angular acceptance was reduced to 7-12 seconds. The sample was positioned in an Eulerian type cradle, where the position optimization of the scattering vector was facilitated by independent variation of the angle of incidence (ω), the diffraction angle (2θ), and the angles of rotation around the surface normal (ψ) and around an in-plane horizontal direction (Ψ). Particularly for the angles ω and 2θ, the position precision in the goniometer, driven by a computer controlled stepper motor system, was 2.5×10^{-4} and 5×10^{-4} degrees, respectively. For all the samples investigated in the present study, a series of ω, ω-2θ and 2θ scans were carried out. RHEED and photoluminescence techniques were used as complementary techniques to confirm the results obtained by the XRD measurements.

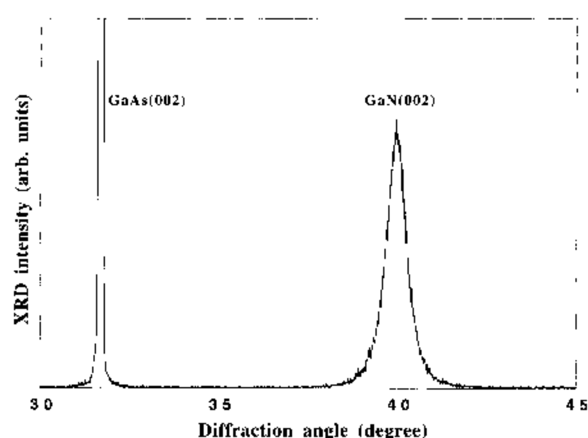

Fig.2 X-ray diffractograph (generated using θ-2θscan) of a GaN epilayer.

§ 3 Results and discussion

3.1 X-ray pole figure analysis on cubic GaN

Figure 2 shows the X-ray diffractograph of a GaN epilayer, grown with an ECR power of 150 Watts, generated using conventional θ-2θ scan. Figure 3 shows the typical high resolution reciprocal space map in the vicinity of the GaN cubic (002) reflection and it is seen that there is no tailing. In addition, the epilayers

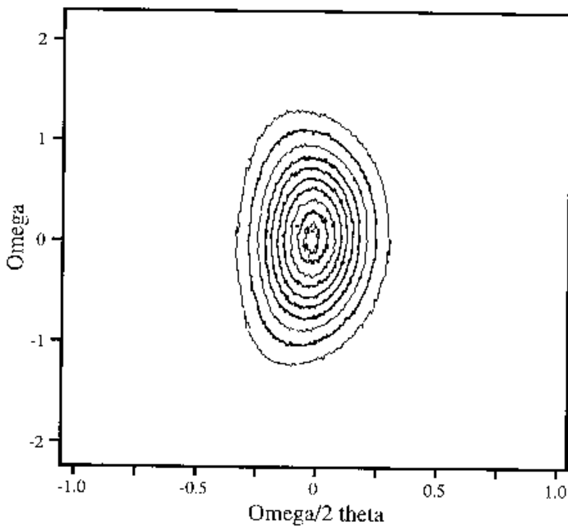

Fig.3 X-ray Reciprocal space map in the vicinity of the cubic GaN (002) reflection.

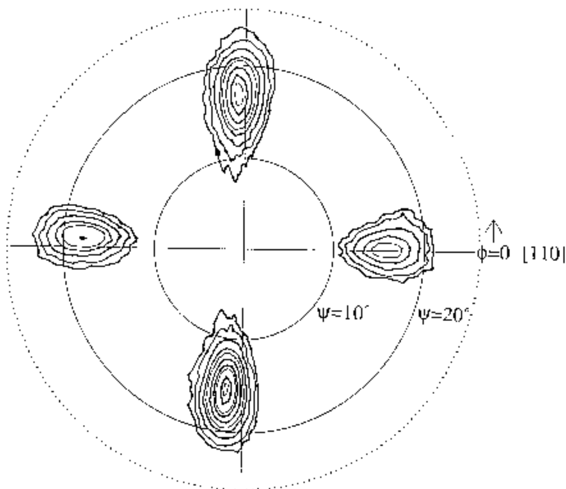

Fig.4 Pole figure of cubic GaN epilayer (obtained for hexagonal (0002) Bragg diffraction condition).

exhibited low temperature luminescence at 3.27 eV, which is the band edge emission of the cubic phase. These results clearly show that the peak in the θ-2θ scan presented in Fig.2 is only due to the cubic (002) phase and not due to any other structural phase such as a hexagonal stacking containing stacking. The diffraction by hexagonal grains could not be recorded in this type of scan. However, this cannot be taken as the evidence for non inclusion of hexagonal grains, because, only the crystallographic planes parallel to the surface could be recorded by θ-2θ scan. Figure 4 shows the pole figure obtained by setting α and 2θ values corresponding to hexagonal (0002) Bragg diffraction of the same sample as Fig.2. The existence of the secondary hexagonal phase is seen in the figure and it exhibits four fold symmetry. The peak positions are found to be inclined by an angle approximately 15.8 degrees from <001> direction. Since hexagonal (0002) and cubic (111) planes have the same interplanar distance, it is very difficult to distinguish from one another. However, it was confirmed that the recorded peaks are due to hexagonal (0002) only and not cubic (111) by settling α and 2θ values corresponding to cubic (002) diffraction and varying y from 0 to 60 degrees. In case it is due to (111) cubic phase, the corresponding cubic (002) peak should appear around 54 degrees. However, in the present case no such peak was observed.

It is interesting to note that the RHEED patterns [Figs. 5(a) and 5(b)] observed during the growth

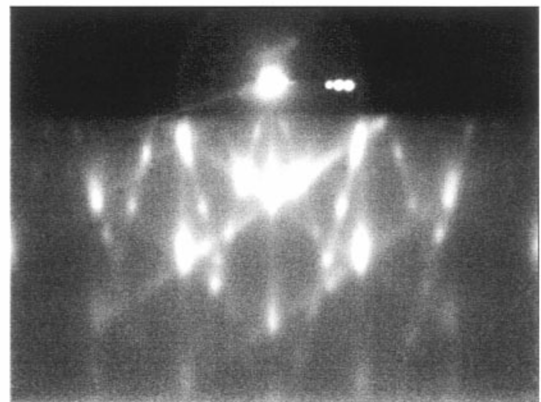

Fig.5(a) RHEED pattern recorded for GaN epilayer during growth.

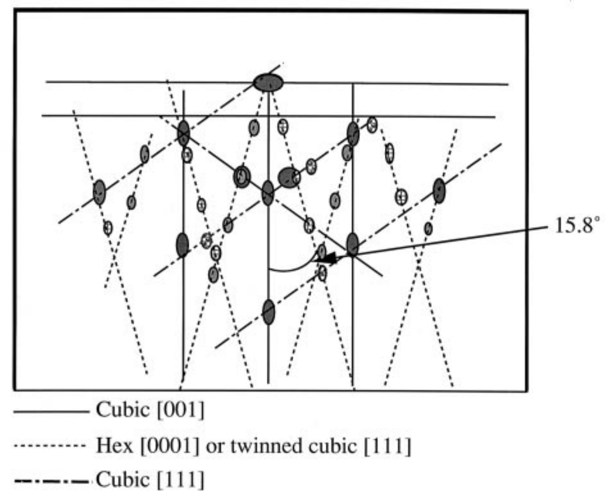

Fig.5(b) Line diagram of the RHEED pattern.

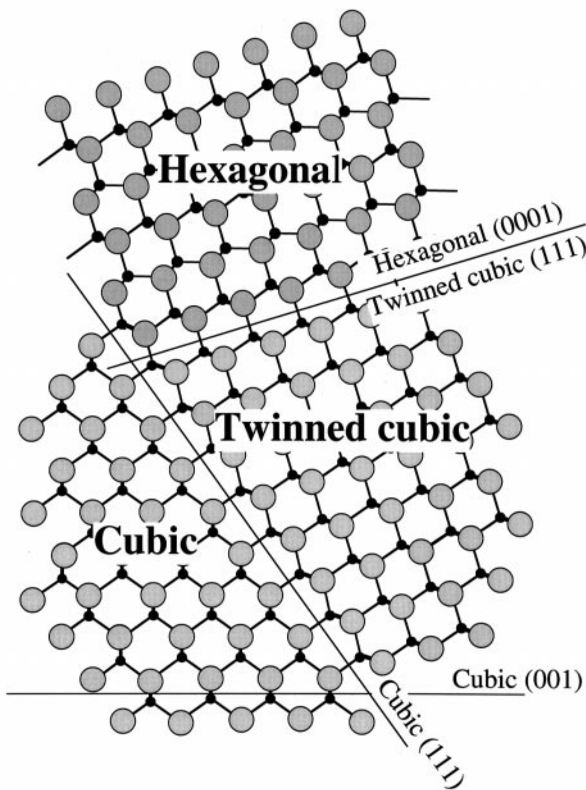

Fig.6(a) Model of growth of hexagonal (0002) phase on twinned cubic GaN.

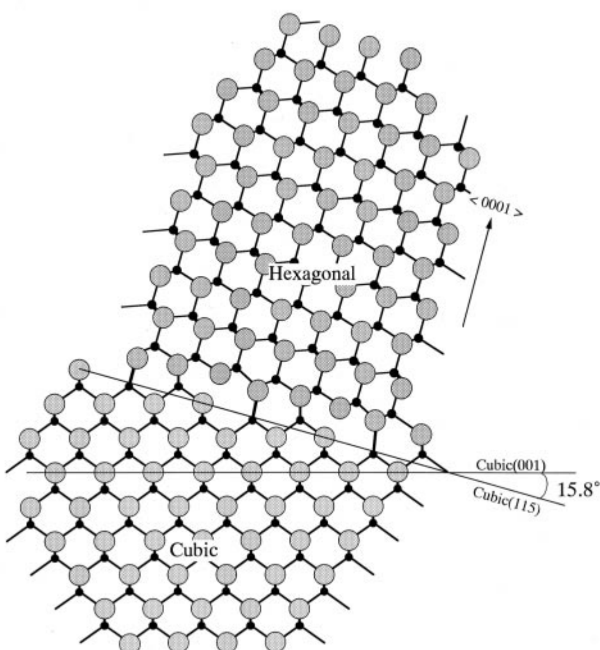

Fig.6(b) Model of growth of hexagonal (0002) phase on GaN (115) facet.

of this epilayer showed additional spot series. RHEED appears to be superposition of three distinct diffraction patterns; the diffraction pattern of <001> oriented cubic crystal observed along <110> direction, and two diffractions either <0001> oriented hexagonal or <111> oriented cubic crystals. These two are inclined by 15.8 degrees from <001> direction. In addition to the above, there is also a series of spots in the direction parallel to cubic <111>. These observations coincide well with XRD results. Sakai et al. have found out that a GaN hexagonal phase grows on {111} cubic planes in the case of GaN growth on GaAs (100) substrates[13]. They also observed stacking faults parallel to {111} planes at the interface between GaN epilayers and GaAs substrates and these stacking faults are responsible for the origination of hexagonal phase. In the present case, we consider that there are two possible origins from where hexagonal grains may have grown. The angle between the (001) surface of the cubic GaN epilayers and their twinned (111) plane is 16 degrees. Since the atomic arrangement of hexagonal (0001) planes is equivalent to that of cubic (111) planes, hexagonal (0001) planes can grow on this 16 degree inclined (111) planes. Therefore the first possibility is this twinned (111) planes [(Fig. 6(a)] as observed by Sakai et al.[13]. The same kind of observation has also been reported by Kuwano et al. for the growth of cubic GaN on (001) GaAs by MOVPE[18]. The second possible origin for the formation of hexagonal phase is GaN {115} facets [Fig.6(b)]. It is seen that there is fairly a good lattice match between (0002) hexagonal plane and cubic (115) facets of GaN. It is also to be noted that the angle between cubic (001) and (115) planes is 15.8 degrees. The presence of hexagonal grains in the lattice of the samples was also verified by photoluminescence measurements.

The hexagonal (0001) phase of GaN is favored to grow on GaAs (111) planes directly due to a good lattice match as discussed by Yamaguchi et al[14]. However in the present investigation, hexagonal GaN was not found to grow on GaAs (111) planes as evidenced by the pole figure measurements. Figure 7 shows the pole figure generated by setting ω and 2θ values corresponding to hexagonal (1010) planes. In case hexagonal phase grows on GaAs (111) planes, then the corresponding (1010) should appear at the Ψ value

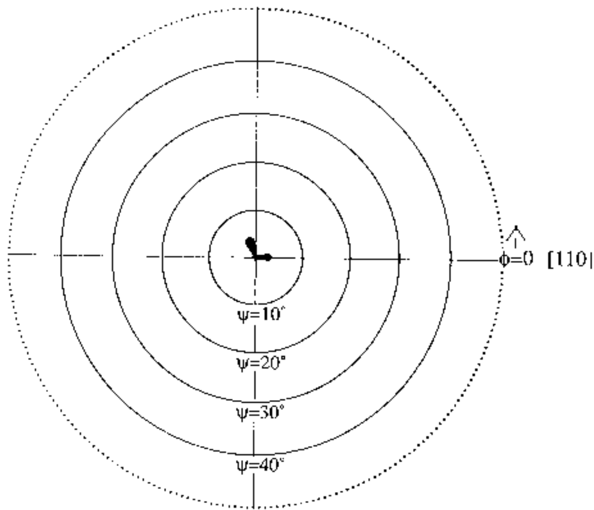

Fig.7 Pole figure of cubic GaN epilayer (obtained for hexagonal (1010) Bragg diffraction condition).

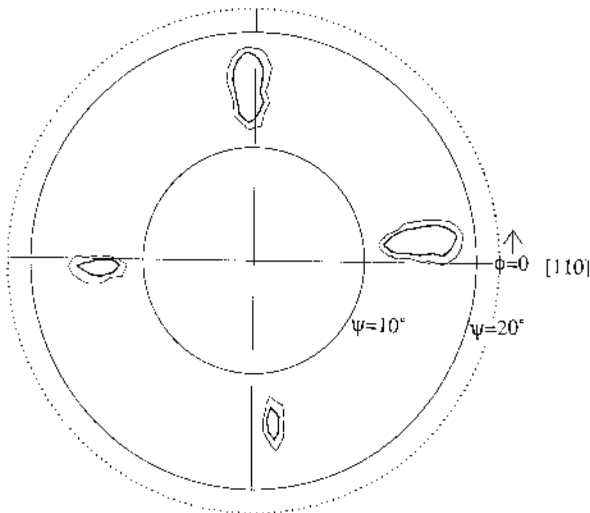

Fig.8 Pole figure of a structurally better cubic GaN epilayer (obtained for hexagonal (0002) Bragg diffraction condition).

Table 1 Structural parameters of GaN

Plane	θ (deg)	Lorentz factor (L)	structure factor (F)	temperature factor (e^{-2M})	
c-(002)	20.0	1.441	74.13	0.94	1.87×10^4
h-(0002)	17.3	1.618	48.25	0.956	4.47×10^4

around 37 degrees. In our case, the intensity of hexagonal (1010) peak was found to be negligible or nil as shown by the pole figure, proving that hexagonal GaN phase has not grown on GaN(111) planes.

For the estimation of actual intensities of hexagonal (0002) and cubic (002) components using the experimentally measured values of diffraction intensities, the integrated intensity calculation was done employing the formula[19,20)]

$$I = I_0 \times |F_{hkl}|^2 \times V \times L \times N^2 \times e^{-2M}$$

where I_0, F, V, L, N and e^{-2M} are the incident X-ray intensity, structure factor, volume factor, Lorentz polarization factor, a number of unit cell per unit volume and temperature factor respectively. The calculated values of the above mentioned parameters for cubic (002) and hexagonal planes (0002) are listed in the Table 1. Using the values of integrated intensities the ratio of the volume contents were calculated. The ratio of hexagonal (0002) to cubic (002) volume contents in this sample was found to be as high as 0.53.

Figure 8 shows the pole figure generated for a structurally superior GaN sample grown with an ECR power of 80 Watts, and it is seen that there is only a little trace of hexagonal phase. The ratio of hexagonal to cubic volume contents for this sample was found to be only 0.02.

As shown above, all the grains oriented in various directions can be easily recorded by generating a pole figure. Pole figures such as these, are very helpful in detecting different structural phases present in a crystal and comparing their relative intensities[21)]. Thus, X-ray pole figure is a very useful tool in identi-

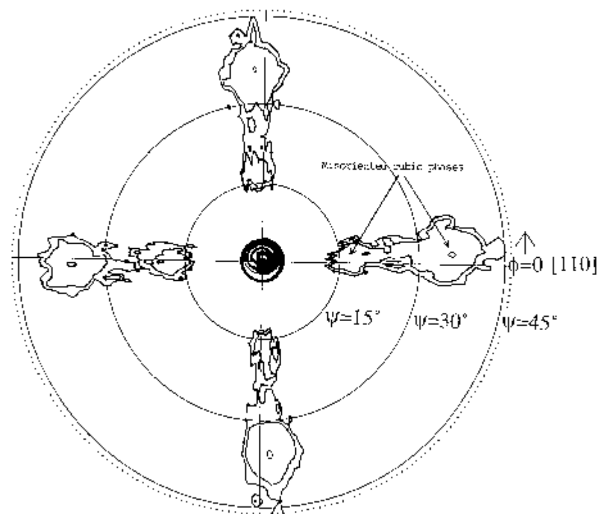

Fig.9 Misoriented cubic phases in the pole figure of cubic GaN (obtained for cubic (004) Bragg diffraction condition) growth of hexagonal (0002) phase on GaN (115) facet.

fying the different phases present and their exact orientations.

Figure 9 shows a pole figure of a cubic GaN epilayer grown on a (001) GaAs substrate obtained by setting ω and 2θ values corresponding to cubic (004) Bragg diffraction. For this sample, the existence of misoriented cubic grains is clearly shown, and the <001> axis of these grains are misoriented by 16.5 and 35.2 degrees from <001> nominal axis, respectively. These grains exhibited four fold symmetry as in the case of secondary hexagonal grains. The intensities of the peaks at two angles were almost the same. This misorientation of the cubic phase may be due to crystal defects or dislocations generated during growth. Sometimes precipitation of the lattice strain due to heteroepitaxial growth also causes this kind of misorientation of strain. On the other hand, typical cubic epilayers on GaAs(001) surfaces, grown using an optimal ECR power, have no such misoriented cubic grains. This kind of misoriented cubic phases can only be recorded by generating pole figures. Sometimes tailing of hexagonal phases present in the epilayers give rise to XRD peaks of this nature[13].

Table 2 HRXRD-FWHM values of hexagonal GaN epilayers grown under different conditions

Growth condition	Omega (arcsec)	2 Theta (arcsec)
Gallium-rich	263	65
Near Equilibrium	290	51
Nitrogen-rich	559	97

3.2 High resolution X-ray diffraction analysis on hexagonal GaN

Figure 10 shows a TEM micrograph of the interface of a typical hexagonal GaN epilayer grown with nitridation as growth initiation. Despite the presence of threading dislocations originating from the interface, epilayers showed excellent structural properties. The layers exhibited columnar structure as observed often in the case hexagonal GaN growth[22-24]. Threading dislocations were found to be the dominant defects

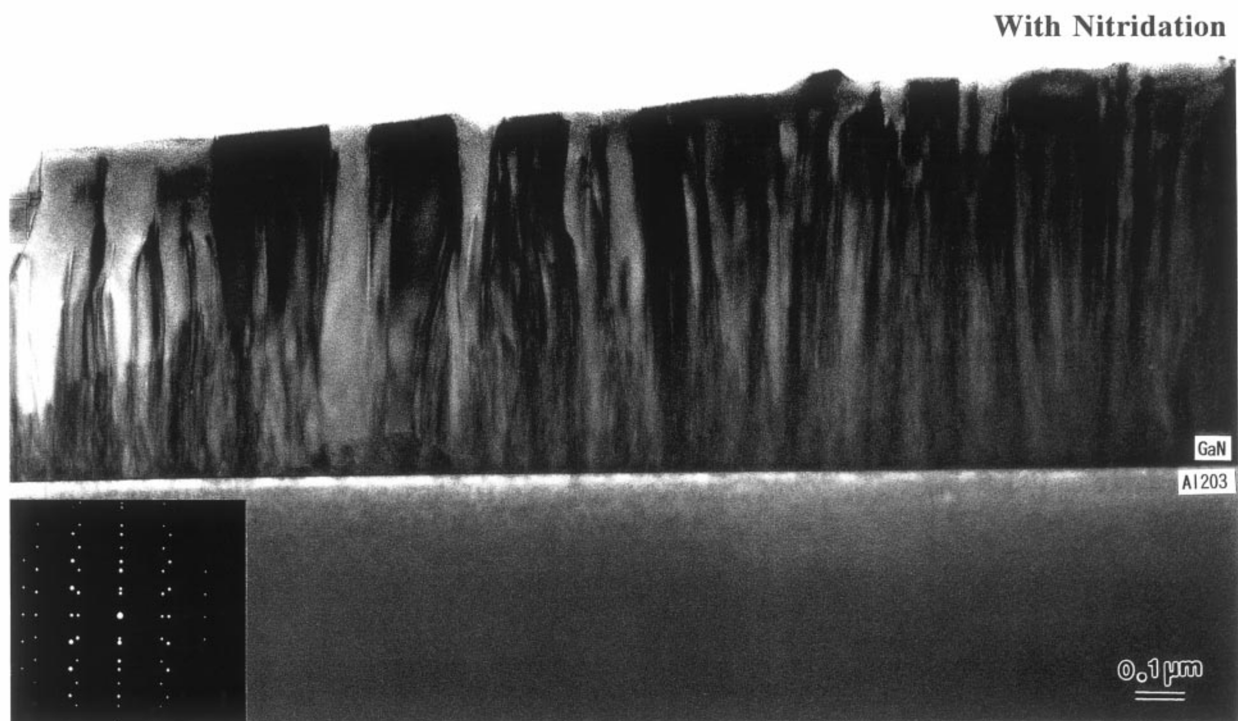

Fig.10 TEM micrograph showing the threading dislocations in the GaN film.

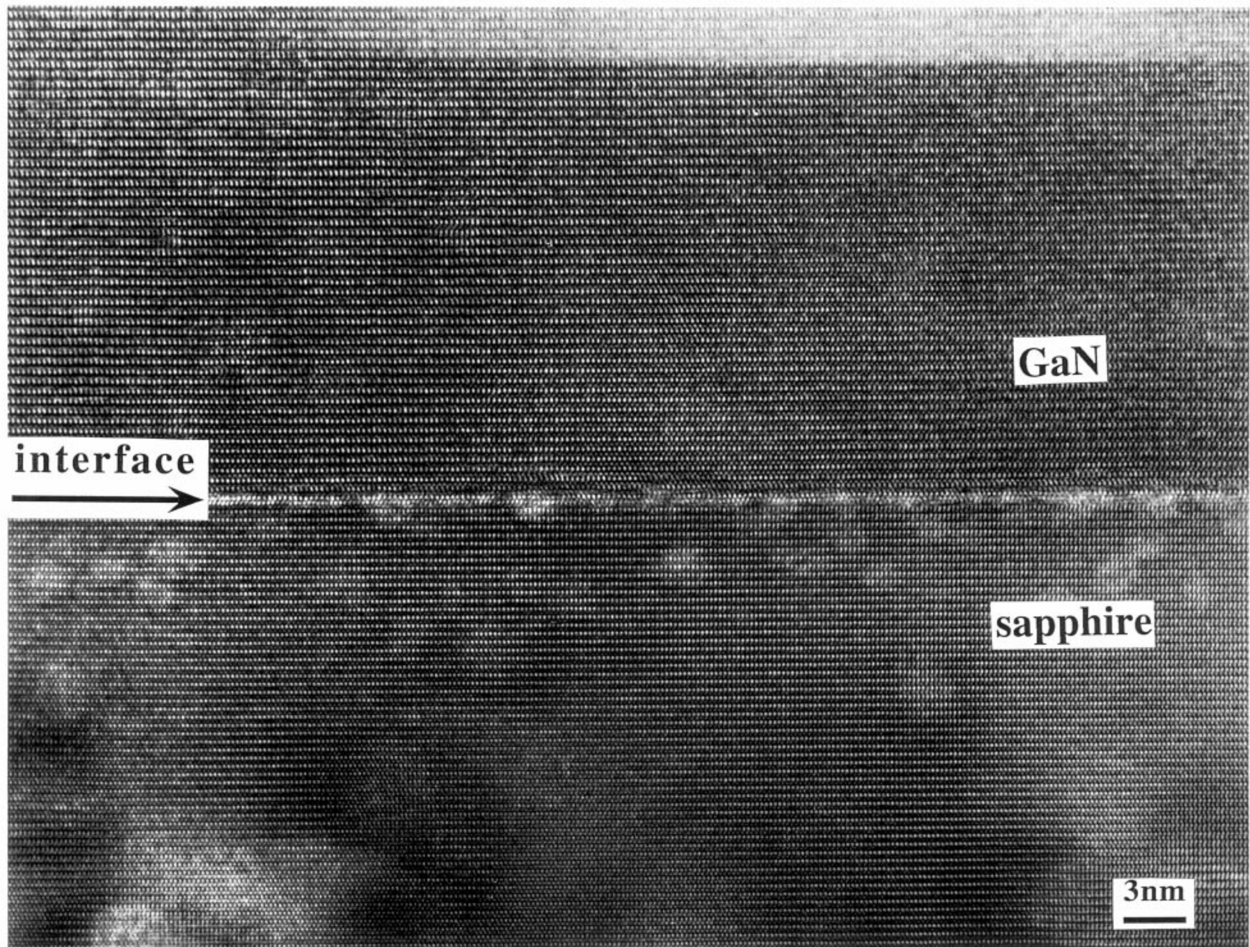

Fig.11 The (0002) receprocal space map of a hexagonal GaN epilayer grown in the equilibrium condition.

and the density was about 10^8 cm^{-2}. However planar defects parallel to the growth direction, such as inversion domains, were hardly found.

High resolution TEM micrograph showed that the interface is completely crystalline and not amorphous. Heating of the substrate at a slow rate of 10°C/min during nitridation lead to a solid phase crystallization of the AlN. This process effectively prevents the formation of basal stacking fault and nanocavities which have been usually observed in the heteroepitaxial growth of GaN[25]. However, in the case of GaN growth with low temperature GaN and AlN buffer layers, these features were found to be present. The defect density of GaN epilayer in the case of growth initiation with nitridation process was found to be in the range of 10^8 cm^{-2}, and it was in the range of 10^{10} cm^{-2} in the case of epilayers grown with the other initiation methods. In general, epilayers grown with other initiation methods, structural properties were found to be substantially poorer when compared with the epilayers grown with nitridation. A comparative analysis of different types of growth initiation of hexagonal GaN epilayers on sapphire has been published elsewhere[4].

Epilayers, approximately of 5μm thickness, grown for 10 hours under different conditions, with nitridation as their initiation, exhibited structural properties as shown in Table 2. As it is seen in the Table, crystal coherence is extremely good whereas there is a large presence of crystal mosaicity in the epilayers of GaN and this is visually distinguished in a typical X-ray reciprocal lattice map generated for an epilayer grown in the near equilibrium condition (Fig.11). The mosaic itself cannot be directly related to dislocation density. In the case of epilayers grown in Ga-rich condition, FWHM is found to be better in the w direction

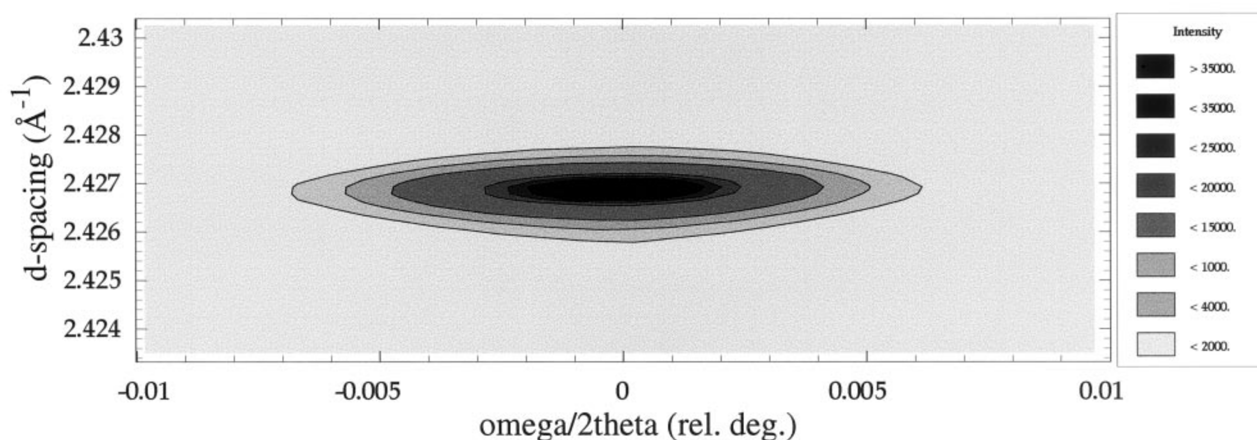

Fig.12 X-ray Receprocal lattice map in the vicinity of the hexagonal GaN (1011) reflection.

than the values estimated for the epilayers grown in the other conditions. This may be due to the major presence of edge dislocations and not the screw or mixed dislocations in the Ga-rich condition. Usually this kind of mixing tends to widen the mosaicity. Edge dislocations slowly get nullified with the increase of thickness of the epilayer by forming loop structures. In the nitrogen rich condition, interface gets relatively rougher than the interfaces in the case of equilibrium and Gallium rich conditions. Also in the nitrogen rich condition both mosaicity and crystal coherence are substantially poorer and it is possibly due to inhomogeneous strain distribution in the lattice and the compositional fluctuations.

Although the epilayers grown with nitridation showed excellent structural properties, electrical properties were found to be surprisingly inferior. In the case of epilayers grown with low temperature AlN buffer layer in addition to substrate nitridation, mobility as high as 147 $cm^2/V.s$ and the carrier concentration of 1.5×10^{17} cm^{-3} were measured. But the structural properties were not found to be good. For a structurally good quality epilayer grown for 2 h with nitridation as growth initiation, hall mobility was measured to be only 60 $cm^2/V.s$. Figure 12 shows a reciprocal lattice map generated in the vicinity of an off-axis plane (1012) for this epilayer. Mosaicity and crystal coherence measured on the (1012) plane (FWHM values were 138 arcsec and 890 arcsec in the 2θ- ω and ω directions, respectively) were found to be substantially poorer than the same parameters measured along the c-direction (57 arcsec and 262 arcsec in the 2θ-ω and w directions, respectively). Different kinds of dislocations originating from the interface due to highly mismatched epitaxy may propagate in different directions and in turn affect the crystalline quality of the off-axis planes. As the thickness increases, structural quality in the c-oriented planes improves. However, the structural quality of the off axis planes was found to be poorer than the c-oriented planes. Threading dislocations were found to meander in different directions as evidenced by TEM micrograph. It is possible that the dislocations get accumulated in the off-axis planes like (1012), (1014) etc. and it turn act as trapping centers for the charge carriers. Multiple buffer layers in addition to substrate nitridation during the initiation of growth may be effective in lowering the propagation of defects into the epilayer.

§ 4 Summary

Structural analysis on cubic GaN by generating X-ray pole figures revealed the presence of misoriented cubic and secondary hexagonal grains. The possible origin of the hexagonal phase is believed to be either twinned cubic (111) planes or cubic (115) facets. X-ray pole figures have been found to be very useful in identifying different structural phases present in the

epilayers and estimating their relative contents. Transmission microscopic analysis revealed the presence of threading dislocation emerging from the interface even for the structurally high quality hexagonal GaN epilayers. However no planar defects parallel to the growth direction were found. Substantial evidences were found by transmission microscopic analysis apart from the X-ray diffraction to prove that the nitridation is the best method for the growth initiation when compared with other low temperature buffer growth techniques from the structural point of view. X-ray diffraction analysis on the off axis planes showed the possible reason for poor electrical characteristics of structurally outstanding materials.

Acknowledgement

K.Balakrishnan acknowledges the receipt of ITIT fellowship awarded by the Agency of Industrial Science and Technology (AIST), Japan.

References:

1) S.Nakamura and G.Fasol, "The Blue Laser Diode - GaN Based Light Emitters and Lasers", Springer, Berlin, 1997.
2) F.A.Ponce and D.P.Bour, Nature **386** (1997) 351.
3) H.Morkoc and S.N.Mohammad, Science **267**(1995)51.
4) K.Balakrishnan, H.Okumura and S.Yoshida, J. Cryst. Growth **189/190**(1998)244.
5) K.Balakrishnan, H.Okumura and S.Yoshida, Proc. 2nd Int. Symp. on Blue Laser and Light Emitting Diodes, pp.634-637, Eds.K.Onabe, K.Hiramatsu, K.Itaya and Y.Nakano.
6) H.Riechert, R.Averbeck, A.Graber, M.Schienle, U. Starub and H. Tews, Mat. Res. Soc. Symp. Proc., **449** (1997) 149, Eds.F.A.Ponce, T.D.Moustakas, I.Akasaki and B.A. Monemar.
7) H.Okumura, H.Hamaguchi, T.Koizumi, K.Balakrishnan, Y.Ishida, M.Arita, S.Chichibu, H.Nakanishi, T.Nagatomo and S.Yoshida, J. Cryst. Growth **189/190** (1998) 390.
8) K.Das and D.K.Ferry: Solid State Electron. **19** (1976) 851.
9) S.Strite and H.Markoc: J.Vac. Sci. Technol. B10 (1992) 1237.
10) C.Y. Yeh, Z.W.Lu, S.Froyen and A.Zunger: Phys. Rev. **B46** (1992) 10086.
11) Y.Xie, Y.Qian, S.Zhang, W.Wang, X.Liu and Y.Zhang: Appl. Phys. Lett., **69** (1996) 334.
12) H.Tsuchiya, K.Sunaba, S.Yonemura, T.Suemasu and F.Hasegawa: Jpn. J. Appl. Phys., **36** (1997) L1.
13) A.Sakai, A.Kimura, H.Sunakawa and A.Usui: Proc.15th Electron. Mat. Symp., '96, Nagoya, Japan, 1996, pp.69.
14) A.A.Yamaguchi, T.Manako, A.Sakai, H.Sunakawa, A.Kimura, M.Nido and A.Usui, Jpn. J. Appl. Phys., **35** (1996) L873.
15) B.Heying, X.H.Wu, S.Keller, Y.Li, D.Kapolnek, B.P.Keller, S.P.DenBaars and J.S.Speck, Appl. Phys. Lett. **68** (1996) 643.
16) Wei Li and Wei-Xin Ni, Appl. Phys. Lett. **68** (1996) 2705.
17) I.P.Nikitina and V.A.Dmitriev, Inst.Phys. Conf. Ser. **141** (1994) 431.
18) N.Kuwano, Y.Nagatomo, K.Kobayashi, K.Oki, S.Miyoshi, H.Yaguchi, K.Onabe and Y.Shiraki: Jpn. J. Appl. Phys. **33** (1994) 18.
19) B.D.Cullity, Elements of "X-ray Diffraction" (Addison-Wesley Publication,USA), 1967.
20) B.E.Warren, "X-ray Diffraction" (Addison-Wesley, Reading, 1969).
21) K.Balakrishnan, G.Feuillet, K.Ohta, H.Hamaguchi, H.Okumura and S.Yoshida, Jpn. J. Appl. Phys. **36** (1997) 6221.
22) M.W.Cole and F.Ren, Appl.Phys. Lett. **71** (1997) 3004.
23) L.T.Romano and T.H.Myers, Appl. Phys. Lett. **71** (1997) 3486.
24) K.Hiramatsu, S.Itoh, H.Amano, I.Akasaki, N.Kuwano, T.Shraishi and K.Oki, J. Cryst. Growth **115** (1991) 628.
25) P.Vennegues, B.Beaumont, M.Vaille and P.Gibart, J. Cryst. Growth **173** (1993) 249.

(Accepted February 12)